Journal of Asian Ceramic Societies 4 (2016) 367–370

Journal of Asian Ceramic Societies

journal homepage: www.elsevier.com/locate/jascer

Electrochromic response of WO_3 and WO_3-TiO_2 thin films prepared from water-soluble precursors and a block copolymer template

Takashi Kuroki, Yuta Matsushima, Hidero Unuma*

Graduate School of Science and Engineering, Yamagata University, 4-3-16 Jonan, Yonezawa, Yamagata 992-8510, Japan

ARTICLE INFO

Article history:
Received 11 May 2016
Received in revised form 11 July 2016
Accepted 17 July 2016
Available online 9 August 2016

Keywords:
Tungsten oxide
Titanium oxide
Electrochromism

ABSTRACT

Electrochromic tungsten trioxide (WO_3) thin films are attracting renewed attention as transmittance-controllable windows for use in automobile, aircraft, and building applications. In order to achieve high electrochromic performance, high cycle stability, and high reliability, the microstructure and compositional homogeneity of WO_3 thin films have to be optimized. In this study, non-doped WO_3 and TiO_2-doped WO_3 thin films were fabricated from water-soluble precursors of tungsten and titanium, and their electrochromic response was investigated. Amorphous WO_3 and TiO_2-doped WO_3 thin films were fabricated by calcining the spin-coated films at 573 K. The use of a PEO-PPO-PEO block copolymer as a porogen facilitated the redox reactions occurring on the thin film/electrolyte interface. Although the effect of TiO_2-doping on the cycle stability of WO_3 thin films has not been fully elucidated, this study demonstrated that TiO_2 doping up to 15 mol% effectively enhanced the cycle stability.

1. Introduction

Tungsten trioxide (WO_3) thin films are potential candidates for use in photochromic devices [1], chemical sensors [2,3], supercapacitors [4], photocatalysts [5], and electrochromic devices [6]. A recent review article [7] describes many practical and potential applications of WO_3 thin films. Electrochromic devices comprising WO_3 thin films have recently attracted renewed attention since they are promising candidates for transmission-controllable windows, i.e., smart windows, which are mounted in modern automobiles, aircrafts, and buildings.

Electrochromism and aforementioned characteristics of WO_3 are a result of the redox reactions between W^{6+} and W^{5+} ions at the WO_3/electrolyte interface, as expressed by Eq. (1)

$$WO_3 + xe^- + xM^+ \leftrightarrow M_xWO_3 \quad (1)$$

where M^+ represents a monovalent cation such as H^+, Li^+, or Na^+. For greater contrast and faster response of an electrochromic WO_3 thin film, reaction (1) needs to proceed at higher rates. Hence, the microstructure of WO_3 thin films has to be optimized to enable faster reaction rates. Among a large variety of methods for fabricating WO_3 thin films including sol–gel [6,8], electrodeposition [9], sputtering [10], hydrothermal [11], and chemical vapor deposition (CVD) [1], liquid-phase deposition of WO_3 from alcoholic [12–14] or aqueous solutions [15,16] seems to be advantageous because it is possible and easy to fabricate porous thin films with micro- or macrosized pores. Highly porous WO_3 thin films have a large surface area for reaction (1) to proceed, implying that they can show a fast electrochromic response and deep contrast in the coloration/bleaching cycles. The most widely used porogens have been polymers such as poly(ethyleneglycol) (PEG) and block copolymers, leading to porous WO_3 thin films with enhanced electrochromic response [12–14,17,18].

Another aspect to be considered for WO_3 thin films is the lifetime or cycle stability. The degradation of the electrochromism of WO_3 thin films upon repeated coloration/bleaching cycles has been attributed to the crystallization of WO_3 and/or $LiWO_3$. TiO_2 doping has long been known to improve the cycle stability of WO_3 thin films [19], believed to occur because the incorporation of TiO_2 hinders the rearrangement of [WO_6] octahedra for crystallization. However, as far as the thin films prepared by liquid-phase deposition techniques are concerned, TiO_2 doping has not necessarily been successful. For example, Lin et al. [20] prepared TiO_2-WO_3 thin films from ethanol solutions of peroxotungstic acid (PTA) and titanium tetra-n-butoxide, $Ti(O\text{-}n\text{-}Bu)_4$, and reported that TiO_2 doping up to 22% elongated the lifetime of WO_3 but slowed the

* Corresponding author. Fax: +81 238 26 3413.
E-mail address: unuma@yz.yamagata-u.ac.jp (H. Unuma).
Peer review under responsibility of The Ceramic Society of Japan and the Korean Ceramic Society.

http://dx.doi.org/10.1016/j.jascer.2016.07.003

electrochromic response. Paipitak et al. [21] prepared TiO_2-WO_3 thin films from aqueous solutions of PTA and Ti(O-n-Bu)$_4$ and found that TiO_2 doping by more than 15% deteriorated the coloration/bleaching contrast. They did not assess the cycle stability. Zayim [22] reported that TiO_2 doping did not improve the cycle stability at all. Other studies on the preparation of TiO_2-WO_3 thin films by liquid-phase deposition did not evaluate the effect of TiO_2 doping on the cycle stability [23,24]. Therefore, the effect of TiO_2 doping has not been fully elucidated. In addition, the effect of TiO_2 doping should be strongly dependent on the process of thin film fabrication.

In this study, WO_3 and WO_3-TiO_2 thin films were prepared from water-soluble precursors of both oxides and a block copolymer as the porogen, and their electrochromic properties and cycle stability were evaluated by cyclic voltammetry and iterative chronoamperometry.

2. Experimental

Non-doped WO_3 thin films were prepared using PTA as the tungsten source and a PEO-PPO-PEO block copolymer (P123, BASF, Ludwigshafen, Germany) as the porogen. PTA was prepared by dissolving approximately 3.0 g of metallic tungsten powder (99.9%, Kojundo Chemical Laboratory, Saitama, Japan) in a mixture of 10 cm^3 of 35% H_2O_2 and 10 cm^3 of pure water at room temperature. The tungsten powder gradually dissolved in the diluted H_2O_2 evolving heat and bubbles to form a transparent, yellow solution. After cooling to room temperature, the supernatant solution was condensed in a rotary evaporator until it became a dry gel. The WO_3 content in the dry PTA gel was determined using a thermogravimetric analyzer (EVO-II, Rigaku, Tokyo, Japan). Typically, the WO_3 content in the PTA gel differed from batch to batch and ranged from 60 to 70 mass%.

P123 was dissolved in water to obtain a concentration of 10.0 mass%. The PTA gel was dissolved in the P123 solution so that the mass ratio of P123:WO_3 varied from 0:100 to 400:100. The formulation details of the coating solutions are shown in Table 1. The non-doped WO_3 thin films prepared from each solution (described later) are denoted as W(x), where x stands for the mass percentage of P123 with respect to that of WO_3, as shown in Table 1.

Glass slides coated with F-doped tin oxide (2 cm × 4 cm) were used as the substrates, which are denoted as FTO substrates. The coating solutions containing PTA and P123 were spin-coated onto the FTO substrates at 1000 rpm for 30 s. The coated substrates were dried at room temperature overnight, and then, calcined at 573 K for 12 h. The heating rate was 1 K/min. The calcination temperature was determined so that P123 was completely burnt off and WO_3 remained amorphous.

TiO_2-doped WO_3 thin films were prepared by substituting 10–40 mol% of WO_3 with TiO_2. For the preparation of TiO_2-doped WO_3 thin films, a water-soluble titanium lactate solution (TC-310, Matsumoto Fine Chemical Co., Ltd., Chiba, Japan), which contained 13.7 mass% TiO_2, was used as the titanium source. The coating solutions were prepared based on the formulation of the solution for W(100). Required amounts of PTA and TC-310 were dissolved in 1.0 cm^3 of the 10.0 mass% P123 solution so that the molar ratio of W:Ti could be varied from 90:10 to 60:40. The solutions were spin-coated on the FTO substrates and calcined in the same manner as the non-doped WO_3 films. The resultant films are denoted as W($1-x$)Ti(x), where x indicates the molar percentage of Ti^{4+}.

The film thickness was measured with a surface profiler (Dektak 3000, Veeco Instruments Inc., NY, USA). The electrochemical properties of the thin films were characterized by cyclic voltammetry and chronoamperometry using a potentio/galvanostat (Versastat 3, Toyo Corp., Tokyo, Japan) at room temperature. In both cases, the electrolyte was propylene carbonate containing 1.0 mol/dm^3 of $LiClO_4$, the counter electrode was a platinum wire, and the reference electrode was a Ag/AgCl pair. The cyclic voltammetry data were recorded at scanning rates of −1.0 to +1.0 V at 50 mV/s. For the chronoamperometry, the potential of the thin films was switched 200 times between −1.0 and +1.0 V at an interval of 5 s.

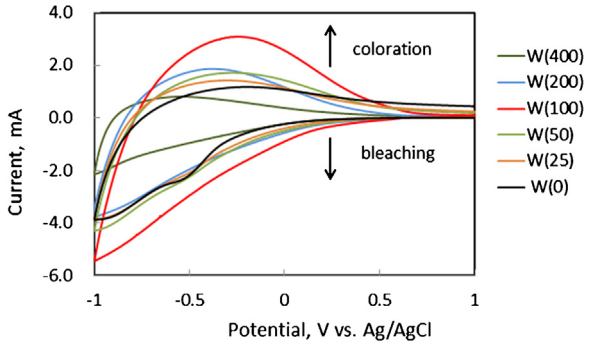

Fig. 1. Cyclic voltammograms of non-doped WO_3 thin films prepared from solutions containing various P123/WO_3 ratios.

3. Results and discussion

3.1. Non-doped WO_3 thin films

Fig. 1 shows the cyclic voltammograms (CVs) of the non-doped WO_3 thin films prepared from solutions containing various P123/WO_3 ratios. The area surrounded by each loop corresponds to the electric charge involved in reaction (1). The as-prepared WO_3 films were colorless, but they became deep blue upon reduction because of the absorption of optical energy in the visible light region through the d-d transition of the 5d electron in the W^{5+} ions. The larger the area of the CV loop, the higher is the contrast. The thickness of the resultant films was 200 ± 30 nm. However, since all the solutions had different viscosities and WO_3 concentrations, the exact thickness and the mass of WO_3 on each substrate may be different for different films. Therefore, the electrochromic properties of "as-prepared" thin films will be compared. W(100) showed the largest CV loop, indicating that W(100) would show the highest electrochromic contrast. The addition of P123 increased the area of the loop from samples W(0) to W(100). It has been well established that polymers added into precursor solutions of thin films can act as porogens and increase surface area [12–14,17,18]. Therefore, in the present case, too, the addition of P123 should have increased the surface area of WO_3 films from W(0) to W(100). However, excessive addition of P123 decreased the area of the CV loops for W(100) to W(400) because of too high a porosity and a decrease in the mass of WO_3 in the film.

Fig. 2(a) and (b) shows the chronoamperograms of the non-doped WO_3 thin films for a single coloration/bleaching cycle. Although the coloration was not complete within 5 s, as indicated by the fact that the current did not return to zero, the bleaching was almost complete within 2 s, as indicated by the currents returning to almost zero. This implies that these WO_3 films showed a relatively fast bleaching response, compared to previous reports in which coloration/bleaching lingered for more than several tens of seconds. The quick response is due to the pores introduced by P123.

Here, the addition of P123 did not result in ordered mesopores, as determined from X-ray diffraction analysis, which was carried out over 2θ angles ranging from 1.5° to 40°. However, non-ordered mesopores were indicated because there was a heap in the low angle region (1.5–3°) (Fig. 3). No diffraction peaks assignable to crystalline WO_3 were observed.

Table 1
The notations for the WO_3 thin films and the formulation of the coating solutions.

Thin film notation	P123 10% solution (cm^3)	Water (cm^3)	WO_3 in PTA (g)	Mass ratio of P123/WO_3
W(0)	0.0	1.0	0.10	0.0
W(25)	0.25	0.75	0.10	0.25
W(50)	0.75	0.25	0.10	0.75
W(100)	1.0	0.0	0.10	1.0
W(200)	1.0	0.0	0.05	2.0
W(400)	1.0	0.0	0.025	4.0

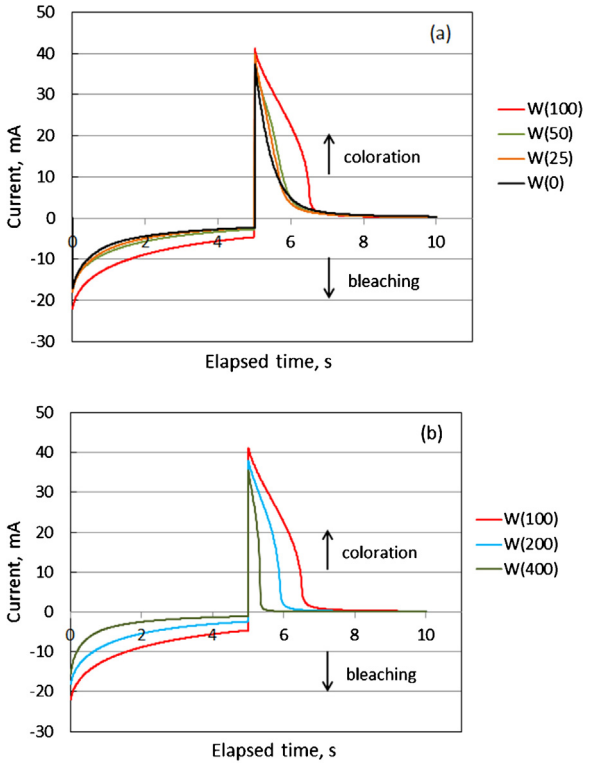

Fig. 2. Chronoamperograms of non-doped WO_3 thin films prepared from solutions containing various P123/WO_3 ratios. The results are shown in two separate drawings to facilitate visualization. (a) shows amperograms for W(0) through W(100), and (b) shows those for W(100) through W(400).

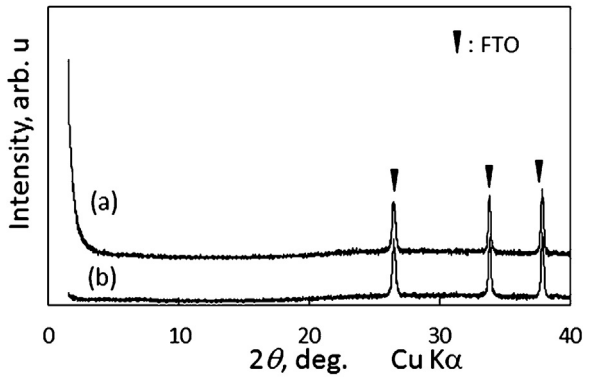

Fig. 3. X-ray diffraction profiles of (a) the W(100) thin film and (b) a FTO-coated substrate, indicating the amorphousness of the W(100) film and suggesting the presence of non-ordered mesopores in the film.

3.2. TiO_2-doped WO_3 thin films

Fig. 4 compares the CVs of TiO_2-doped WO_3 thin films. The CV of non-doped W(100) is also shown for comparison. The addition of TiO_2 did not necessarily decrease the area of the loop. This is

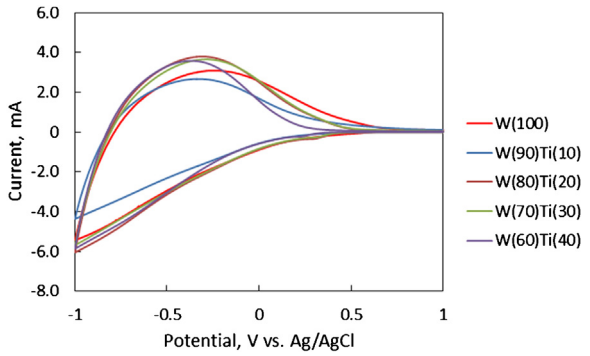

Fig. 4. Cyclic voltammograms of TiO_2-WO_3 thin films and the W(100) film.

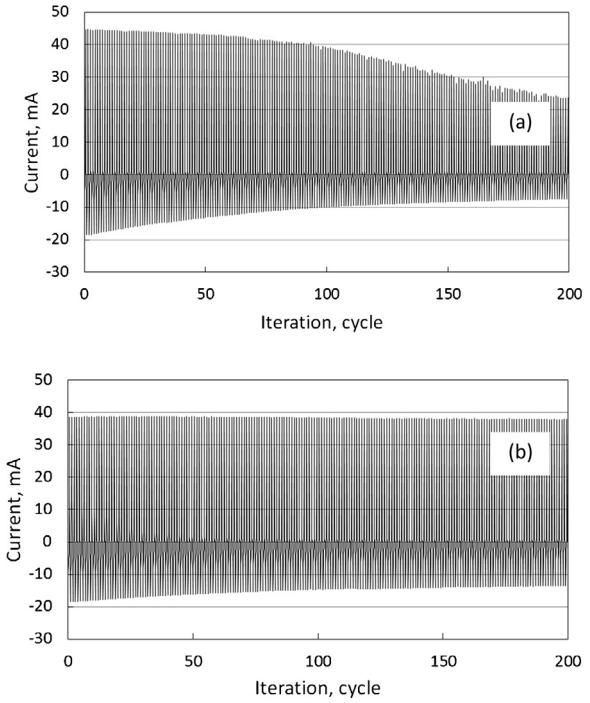

Fig. 5. Iterative chronoamperograms of (a) W(100) and (b) W(90)Ti(10) thin films.

not because Ti^{4+} participated in the redox reaction but because the addition of TiO_2 somewhat increased the film thickness or porosity. TiO_2 doping has a more pronounced effect on the cycle stability, as shown in Fig. 5. The cycle stability of non-doped W(100) thin film upon repeated coloration/bleaching was poor because both coloration and bleaching currents decreased with increasing iteration cycle [Fig. 5(a)]. However, a W(90)Ti(10) thin film containing 10 mol% TiO_2 showed only a small decrease in the current [Fig. 5(b)]. The stability upon repeated coloration/bleaching of all the TiO_2-doped thin films and non-doped W(100) thin film is summarized in Fig. 6. In this figure, the peak coloration and bleaching currents at every 20 cycles were recorded from the iterative

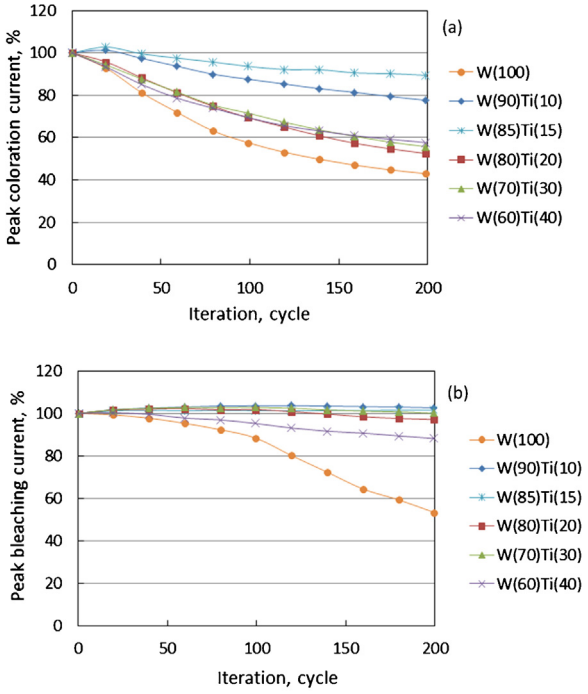

Fig. 6. Change in peak currents of (a) coloration and (b) bleaching after every 20 cycles.

chronoamperometry, as is shown in Fig. 5, and normalized with respect to the peak coloration and bleaching currents in the first cycle. This figure indicates that the coloration and bleaching response of the non-doped W(100) thin film decreased to 40–50% after 200 cycles, while TiO_2 doping suppressed the degradation of the currents. In particular, TiO_2 doping by 15 mol% suppressed the degradation of the currents most effectively. Extensive doping by more than 20 mol% was not effective for improving cycle stability [W(80)Ti(20) to W(60)Ti(40)].

As described above, TiO_2 doping of liquid-phase-deposited WO_3 was not necessarily successful at improving the electrochromic contrast and cycle stability [20–22]. One possible explanation for this is that the distribution of Ti^{4+} may not be homogeneous in the WO_3 matrix since the reactivity of the titanium alkoxides and the tungsten precursors are not identical. In contrast, we used water-soluble titanium lactate solution as the titanium source. That should make it possible for a more homogeneous distribution of Ti^{4+} in the WO_3 matrix to be achieved, and effectively stabilize against degradation during the coloration/bleaching cycles.

4. Conclusions

Non-doped WO_3 and TiO_2-doped WO_3 thin films were prepared from water-soluble precursors of tungsten and titanium. Aqueous solutions of PTA and titanium lactate containing a PEO-PPO-PEO block copolymer were spin-coated on glass slides coated with F-doped tin oxide, and then, the dried films were calcined at 573 K to obtain amorphous thin films. The use of the block copolymer facilitated the redox reactions between W^{6+} and W^{5+} on the thin film/electrolyte interface through, most probably, the generation of mesopores in the thin films. The effect of TiO_2-doping on the coloration/bleaching cycle stability was systematically investigated, and it was determined that TiO_2-doping by up to 15 mol% effectively enhanced the cycle stability.

References

[1] R.G. Palgrave and I.P. Parkin, J. Mater. Chem., 14, 2864–2867 (2004).
[2] Y. Wang, X. Cui, Q. Yang, J. Liu, Y. Gao, P. Sun and G. Lu, Sens. Actuators B: Chem., 225, 544–552 (2016).
[3] W.-C. Hsu, C.-C. Chen, C.-H. Peng and C.-C. Chang, Thin Solid Films, 516, 407–411 (2007).
[4] R. Yuksel, C. Durucan and H.E. Unalan, J. Alloys Compd., 658, 183–189 (2016).
[5] H. Yoon, M.G. Mali, M. Kim, S.S. Al-Deyab and S.S. Yoon, Catal. Today, 260, 89–94 (2016).
[6] J. Livage and D. Ganguli, Sol. Energy Mater. Sol. Cells, 68, 365–381 (2001).
[7] H. Zheng, J.Z. Ou, M.S. Strano, R.B. Kaner, A. Mitchell and K. Kalantar-zadeh, Adv. Funct. Mater., 21, 2175–2196 (2011).
[8] H. Unuma, K. Tonooka, Y. Suzuki, T. Furusaki, K. Kodaira and T. Matsushita, J. Mater. Sci. Lett., 5, 1248–1250 (1986).
[9] S.-H. Baeck, K.-S. Choi, T.F. Jaramillo, G.D. Stucky and E.W. McFarland, Adv. Mater., 15, 1269–1273 (2003).
[10] N. Janke, A. Bieberle and R. Weißmann, Thin Solid Films, 392, 134–141 (2001).
[11] V.V. Kondalkar, S.S. Mali, R.R. Kharade, K.V. Khot, P.B. Patil, R.M. Mane, S. Choundhury, P.S. Patil, C.K. Hong, J.H. Kim and P.N. Bhosale, Dalton Trans., 44, 2788–2800 (2015).
[12] W. Cheng, E. Baudrin, B. Dunn and J.I. Zink, J. Mater. Chem., 11, 92–97 (2001).
[13] E. Ozkan, S.-H. Lee, P. Liu, C.E. Tracy, F.Z. Tepehan, J.R. Pitts and S.K. Deb, Solid State Ionics, 149, 139–146 (2002).
[14] Y. Zhang, J. Yuan, J. Le, L. Song and X. Hu, Sol. Energy Mater. Sol. Cells, 93, 1338–1344 (2009).
[15] J. Livage and G. Guzman, Solid State Ionics, 84, 205–211 (1996).
[16] A. Patra, K. Auddy, D. Ganguli, J. Livage and P.K. Biswas, Mater. Lett., 58, 1059–1063 (2004).
[17] E.O. Zayim, P. Liu, S.H. Lee, C.E. Tracy, J.A. Turner, J.R. Piits and S.K. Deb, Solid State Ionics, 165, 65–72 (2003).
[18] Y. Djaoued, P.V. Ashrit, S. Badilescu and R. Brüning, J. Sol-Gel. Sci. Technol., 28, 235–244 (2003).
[19] S. Hashimoto and H. Matsuoka, Surf. Interface Anal., 19, 464–468 (1992).
[20] C.-L. Lin, Y.-W. Chen and E. Chen, Thin Solid Films, 556, 48–53 (2014).
[21] K. Paipitak, C. Kahattha, W. Techitdheera, S. Porntheeraphat and W. Pecharapa, Energy Procedia, 9, 446–451 (2011).
[22] E.O. Zayim, Sol. Energy Mater. Sol. Cells, 87, 695–703 (2005).
[23] M. Yuan, Y. Lu, B. Tian, H. Yang, B. Tu, J. Kong and D. Zhao, Chem. Lett., 33, 1396–1397 (2004).
[24] Z. Wang and X. Hu, Electrochim. Acta, 46, 1951–1956 (2001).